Available online at www.sciencedirect.com
SCIENCE DIRECT
Cement and Concrete Research 36 (2006) 137–143
Cement and Concrete Research

Long-term performance of cement paste during combined calcium leaching–sulfate attack: kinetics and size effect

D. Planel[a], J. Sercombe[b,*], P. Le Bescop[b], F. Adenot[c], J.-M. Torrenti[d]

[a]Centre d'Etudes et de Recherches de l'Industrie du Béton, Département Matériaux, Laboratoire Microstructure, BP 59, 28231 Epernon Cedex, France
[b]Atomic Energy Commission, Laboratoire d'Etude du Comportement des Bétons et des Argiles, 91191 Gif-sur-Yvette, France
[c]Atomic Energy Commission, Laboratoire d'Étude du Comportement Physico-chimique des Colis, 13108 Saint-Paul-Lez-Durance, France
[d]Ecole Nationale des Ponts et Chaussée, Cité Descartes, 77455 Marne-La-Vallée Cedex 2, France

Received 8 August 2003; accepted 28 July 2004

Abstract

This paper presents experimental results obtained on cement paste samples (water/cement ratio of 0.4) subjected to a low-concentration (15 mmol/l) external sulfate attack during several weeks. Chemical and microstructural analyses include the continuous monitoring of calcium loss and sulfate consumption within the cement paste, periodic layer by layer X-ray diffraction (XRD)/energy-dispersive spectrometer (EDS) analyses of the solid constituents of the cement matrix (ettringite, portlandite, gypsum) within the calcium-depleted part of the samples. Scanning electron microscopy (SEM) and visual observations are used to follow the crack pattern evolution during the external sulfate attack. The relation between the size of the specimen and crack initiation/development is investigated experimentally by performing tests on samples with different thickness/diameter ratios.

Keywords: Cement paste; Long-term performance; Sulfate attack; Ettringite; Microcracking

1. Introduction

This paper is concerned with the assessment of the durability performance of concrete in nuclear waste containment. Calcium leaching of cement paste under deionized water, considered as the reference scenario of chemical degradation in this context, is characterized in particular by the dissolution of portlandite ($Ca(OH)_2$) and the decalcification of Calcium Silica Hydrates (C–S–H), leading to the diffusion of calcium ions towards the outside medium [1–3]. In realistic site conditions for nuclear waste storage, sulfate ions are expected in low quantities (<7–31 mmol/l [4]). Durability of concrete in sulfate environment is therefore of great concern. External sulfate attack of cementitious materials is in itself a well-documented phenomenon. Some notable recent reviews on the subject are, among others, those by Cohen and Mather [5], Mehta [6,7], and Brown and Taylor [8]. Sulfate attack can lead to significant mechanical damage (cracking), related mainly to differential internal expansions, caused, according to the literature, primarily by ettringite formation and secondly by gypsum. The development of cracking greatly depends on the geometry and size of the tested specimen [11]. Under controlled external conditions (constant pH and sulfate concentration), the weakening of the material related to calcium leaching [9,10] (portlandite and C–S–H decomposition) should also be taken as part of sulfate attack mechanisms, according to Refs. [12,14]. The relative importance of calcium leaching, with regards to the overall damage of cementitious materials during external sulfate attack, has not, however, been studied in details.

In this paper, experimental results are presented concerning low concentration sodium sulfate attack of portland cement paste (15 mmol/l and constant pH of 7) and compared with that obtained on the same cement paste

* Corresponding author. CEA Cadarache, DEN/DTCD/SPDE/L2ED—Bât 163, 13108 Saint-Paul-Lez-Durance Cedex, France. Tel.: +33 4 42 25 30 72; fax: +33 4 42 25 46 15.
E-mail address: sercombe@cea.fr (J. Sercombe).

0008-8846/$ - see front matter © 2004 Elsevier Ltd. All rights reserved.
doi:10.1016/j.cemconres.2004.07.039

immersed in pure deionized water. Periodic chemical and layer-by-layer X-ray diffraction (XRD)/energy-dispersive spectrometer (EDS) microstructural investigations are performed in order to follow the rate, intensity and depth of penetration of sulfate attack. This methodology is similar to that used in standard calcium leaching tests [2,3] to follow the calcium depleting of the material and has scarcely been applied to internal [13] or external sulfate attack [14]. The kinetics of progression of dissolution/precipitation fronts (portlandite, ettringite, and gypsum) during the tests can by this way be assessed. By performing tests on specimens of different thickness, size effects are furthermore studied. These results are of great importance for the development of coupled diffusion-transport and chemical models needed to predict the service life of structures submitted to sulfate attack.

2. Experimental program

2.1. Materials

To obtain results in short times and enhance the phenomena, a non sulfate-resistant cement was chosen, the CPA–CEM I 52.5 R NF. Its high gypsum (5.7%) and C_3A (10.5%) contents together with a high surface area (S_{Blain}=440 m^2/kg) ensured its potential reactivity to sulfates [5]. Its chemical composition is given in Table 1. Cement paste samples with a water/cement ratio of 0.4 were cast in cylindrical moulds 7 cm in diameter and 10 cm in height. Curing at 100% relative humidity and constant temperature (20 °C) lasted for 28 days. Cylinders were then cut in 4-, 8-, 16-, and 32-mm-thick slices and were kept in sealed bags and nitrogen atmosphere to avoid carbonation.

2.2. Experimental setup

The experimental setup consisted of cylindrical tanks for standard calcium leaching tests, as described in Fig. 1. In all the tests, the pH and temperature were kept constant, respectively, at 7 and 20 °C. Nitric acid at a concentration of 1 mol/l was added automatically to the solutions to regulate the pH. To avoid carbonation of the samples during the tests, nitrogen gas was continuously injected in the tanks. Cylindrical slices, 4-, 8-, 16-, and 32-mm thick, of cement paste were immersed in a 30-l tank filled with a solution of Na_2SO_4 at 15 mmol/l. The samples were protected from lateral degradation by an epoxy coating, such that the external attack occurred in one direction only, perpendicular to the circular faces. To maintain experimental conditions constant during the tests, the solution was renewed at regular intervals, in connection with the quantity of added nitric acid. In fact, this quantity is directly related to the amount of calcium leached from the cement paste, as it is the case for calcium leaching in pure deionized water [2]. By this way, almost constant sulfate and calcium concentrations of 15 and 0 mmol/l, respectively, could be ensured throughout the test. The solutions were constantly stirred to avoid any local increase of concentration. To follow precisely the evolution of the leachant (outward and inward fluxes), a 4-mm-thick slice was also immersed in a 2-l cylindrical tank filled with the sodium sulfate solution (with a similar control of the pH and regular renewing).

To compare the results obtained on samples subjected to sulfate attack with that relative to standard calcium leaching tests, a reference set of cylindrical slices, 4-, 8-, 16-, and 20-mm thick, was immersed in pure deionized water, with pH regulation and renewing at regular intervals to avoid any increase of the calcium concentration in the solution. A 4-mm-thick slice was also placed in a 2-l tank filled with pure deionized water to analyze the evolution of the leachant. As pointed out by Refs. [15–17], the adequate control of external conditions (pH and concentrations) significantly increases the rate of sulfate attack. This result is probably related to the accelerated rate of calcium leaching in this case, as shown by Refs. [3] for tests performed in pure deionized water. It is therefore important to ensure a similar control of external conditions for the reference set, if meaningful comparison is expected.

Table 1
Chemical composition (in percent (%) of mass) of CPA–CEM I 52.5 R cement

CaO	SiO_2	Al_2O_3	SO_3	Na_2O
64.4	20.4	5.2	3.7	0.1

3. Experimental results

To understand the underlying chemo-physical processes occurring during the combined calcium leaching–sulfate attack tests, information were required concerning: 1) the ionic quantities and their diffusion inward and outward from the cement paste, 2) the solid compounds initially in the cement paste or formed during the tests. To this end, chemical analyses of the sulfate sodium solution at regular intervals provided some insight on the outward fluxes of calcium and hydroxyl ions and the inward flux of sulfate ions. X-ray diffraction (XRD), scanning electron microscopy (SEM) and energy-dispersive spectrometer microanalyses (EDS) were used to determine the mineralogy of the calcium depleted (which defines the degraded layer) and sound layers of the cement paste samples. The results of these analyses together with visual observations and crack patterns are presented hereafter.

3.1. Size effect

Depending on the thickness of the cylindrical samples, the onset of cracking occurred at different times. The evolution and the distribution of cracks were however

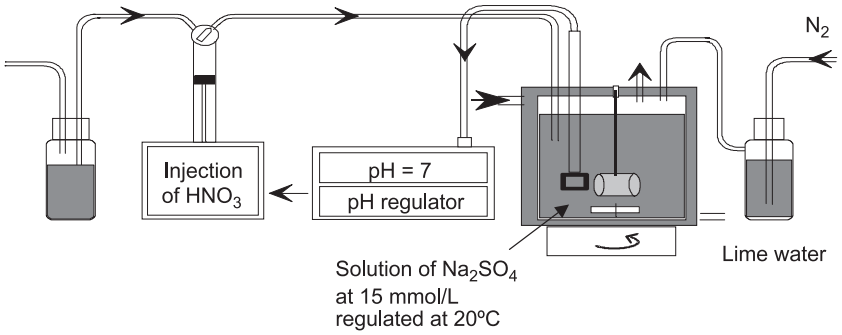

Fig. 1. Experimental setup for sulfate attack tests on cement paste.

almost similar for all the specimen (only the 4-mm-thick specimen showed surface delamination before failure). It consisted in cracks perpendicular to the leached surfaces (see Fig. 2), which developed rapidly and lead to the breakdown of the samples within a few days (cracks were therefore not restricted to the outer decalcified layer of the samples). Once failure of the samples was achieved, further cracks appeared parallel to the leached surface, leading to surface spalling, as found by Ref. [18] for similar tests at higher sodium sulfate concentrations. The durations of immersion leading to the initiation of cracking (which define the "crack initiation times"), as determined visually, are plotted in Fig. 3 in function of the samples thickness. The duration of the cracking process, that is to say, the time interval between crack initiation and structural failure of the samples (breakdown) is also given in Fig. 3. Obviously, this interval remains very small, whatever the size of the specimen and reflects the brittle nature of cement paste when subjected to tensile stresses. According to the results of Fig. 3, the "crack initiation time" appears to be proportional to the thickness with a stabilization of the curve for thick samples, as shown by the polynomial regression. No cracks were observed on the reference set of cement paste samples immersed in pure deionized water.

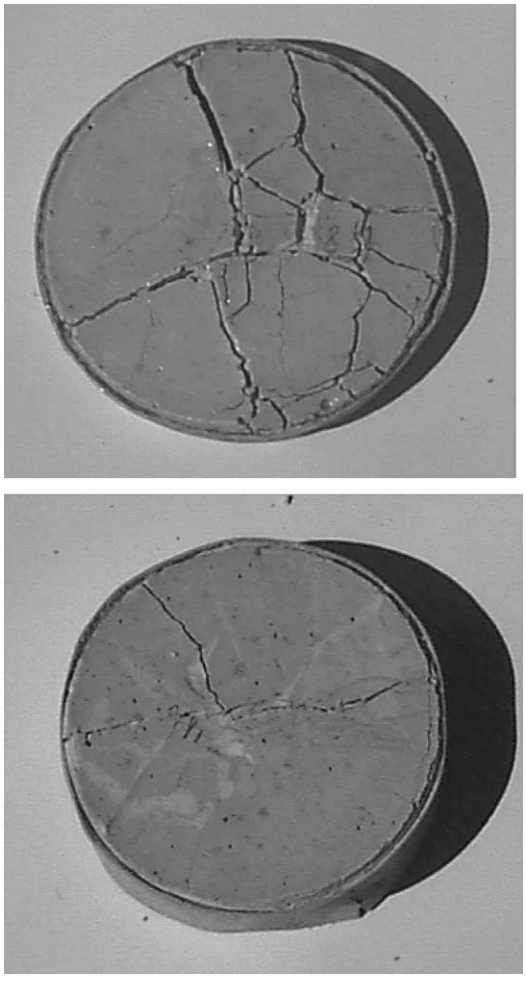

Fig. 2. Cement paste samples, 8- and 16-mm thick after failure.

3.2. Chemical analyses of the leachant

Fig. 4 shows the cumulative quantities of OH^-, Ca^{2+}, and SO_4^{2-} ions obtained by ionic chromatography, as a function of the square root of time for the 4-mm-thick specimens tested in the sulfate sodium solution (Na_2SO_4) and in pure water (H_2O). All the measures were performed till the onset of cracking. The slope of the fluxes in the sulfate attack test are, respectively, 2.6 mol/m^2/days$^{0.5}$ for OH^-, 1.1 mol/m^2/days$^{0.5}$ for Ca^{2+} and −0.4 mol/m^2/days$^{0.5}$ for SO_4^{2-}. Positive fluxes refer to outward fluxes while negative fluxes correspond to inward fluxes. Calcium and Hydroxyl ions result mainly from the dissolution of

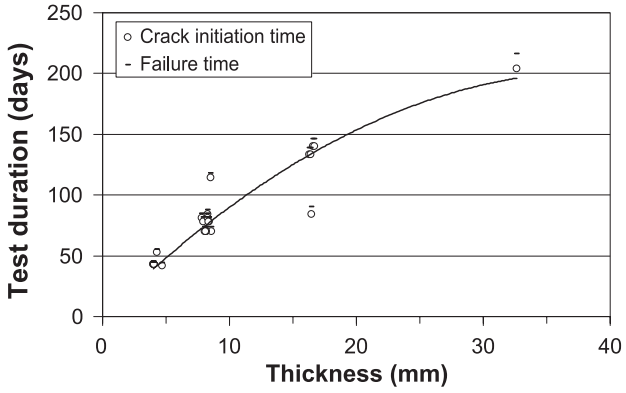

Fig. 3. Test duration in function of the thickness of the cement paste samples.

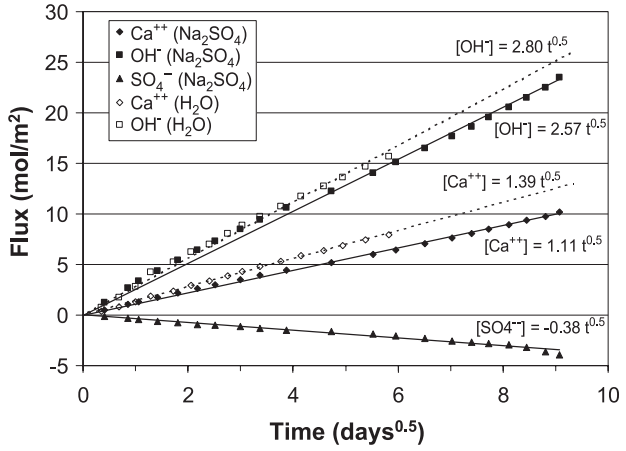

Fig. 4. Inward and outward fluxes of calcium, hydroxyl and sulfate ions during the sulfate attack test (Na_2SO_4) and the calcium leaching test in pure deionized water (H_2O).

portlandite ($Ca(OH)_2 \leftrightarrow Ca^{2+}+2OH^-$) and to a lesser extent from the calcium depleting of C–S–H [3,18]. The consumption of sulfates between two renewing of the sodium sulfate solution represents about 10% of the initial content of the solution. For calcium leaching in pure deionized water, considered in this study as the reference scenario, the ratio between hydroxyl and calcium fluxes is equal to 2 (2.8 mol/m^2/days$^{0.5}$ for OH^- and 1.4 mol/m^2/days$^{0.5}$ for Ca^{2+}), reflecting mainly the dissolution of portlandite. As pointed out by Refs. [2,3,8], these results demonstrate that charge balance in the pore solution is maintained essentially by outward migration of OH^-. This ratio is, however, not quite equal to 2 during the sulfate attack test. While the fluxes of hydroxyl ions are almost identical in the two tests, the slope of the calcium flux during the sulfate attack test (1.1 mol/m^2/days$^{0.5}$) is 25% smaller than that obtained for leaching in pure water (1.4 mol/m^2/days$^{0.5}$). As shown hereafter, this could be a consequence of the calcium consumption related to internal precipitation of gypsum and ettringite.

3.3. Mineralogy of the leached zone

The mineralogy of the leached zone was assessed by scraping progressively the cylindrical samples from the external surface to the center of the slices. With the help of XRD (X-ray diffraction) analyses, it was possible by this way to determine the solid compounds within slices of less than 100-μm thick, parallel to the leached surface. By using this methodology at different times, the complete mineralogy of the material is obtained, together with the evolution of precipitation fronts (ettringite, gypsum) and dissolution fronts (portlandite). To obtain profiles without any perturbations related to cracking, samples of different thickness were used. As soon as cracks were observed on a sample of a given thickness, an uncracked sample with a thickness twice that of the cracked sample was removed from the solution and readily scraped. Conservation of the obtained solid powders before XRD analyses was achieved in nitrogen-controlled atmosphere to avoid carbonation. Three X-ray diffraction angles (CuKα, 2θ) were used to characterize the phases: ettringite at 9.1, gypsum at 20.8, and portlandite at 34.1. The peak at 20.8 for gypsum was chosen rather than 29.2 to avoid confusion with calcite $CaCO_3$ (29.3). The heights of the peaks in the different layers were taken as estimates of the amount of the phases. The resulting profiles obtained on samples tested during 5 weeks (corresponding to the onset of cracking for the 4-mm-thick slices), 10 weeks, 12 weeks (corresponding to the onset of cracking for the 8-mm-thick slices), and 20 weeks (corresponding to the onset of cracking for the 16-mm-thick slices) in the sodium sulfate solution are presented in Fig. 5. The vertical scale for each date is identical, with a maximum intensity of 35 counts/s. These profiles show the existence of three distinct layers:

- zone 1 where ettringite (AFt) appears to be qualitatively the dominant crystallized phase and where calcium hydroxide ($Ca(OH)_2$) is completely dissolved,
- zone 2 in which portlandite coexist with ettringite (AFt) and gypsum ($CaSO_4$, $2H_2O$). This zone is of reduced thickness,
- zone 3 in which the cement paste contains portlandite ($Ca(OH)_2$) in important quantities. This allows to define as for calcium leaching in pure deionized water [2] a sound zone (where no calcium depletion has taken place) and a calcium-depleted thickness (based on the dissolution of portlandite only, without any considerations of C–S–H).

Many authors report that external sulfate attack on a paste or mortar proceeds through the advance of a reaction front into the material [14,18,19], with the presence of gypsum and ettringite layers. It is generally admitted that gypsum precipitation occurs close to the attacked surface because its formation requires higher sulfate concentrations than that of ettringite. The profiles of Fig. 5 show on the

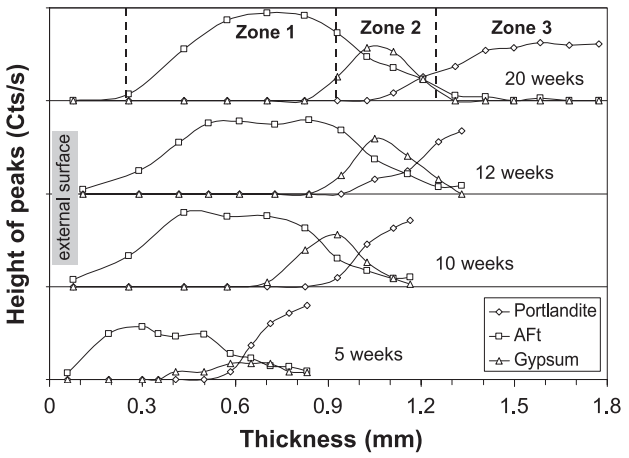

Fig. 5. Phase distribution at different times in the calcium depleted zone of the cement paste samples immersed in the sodium sulfate solution.

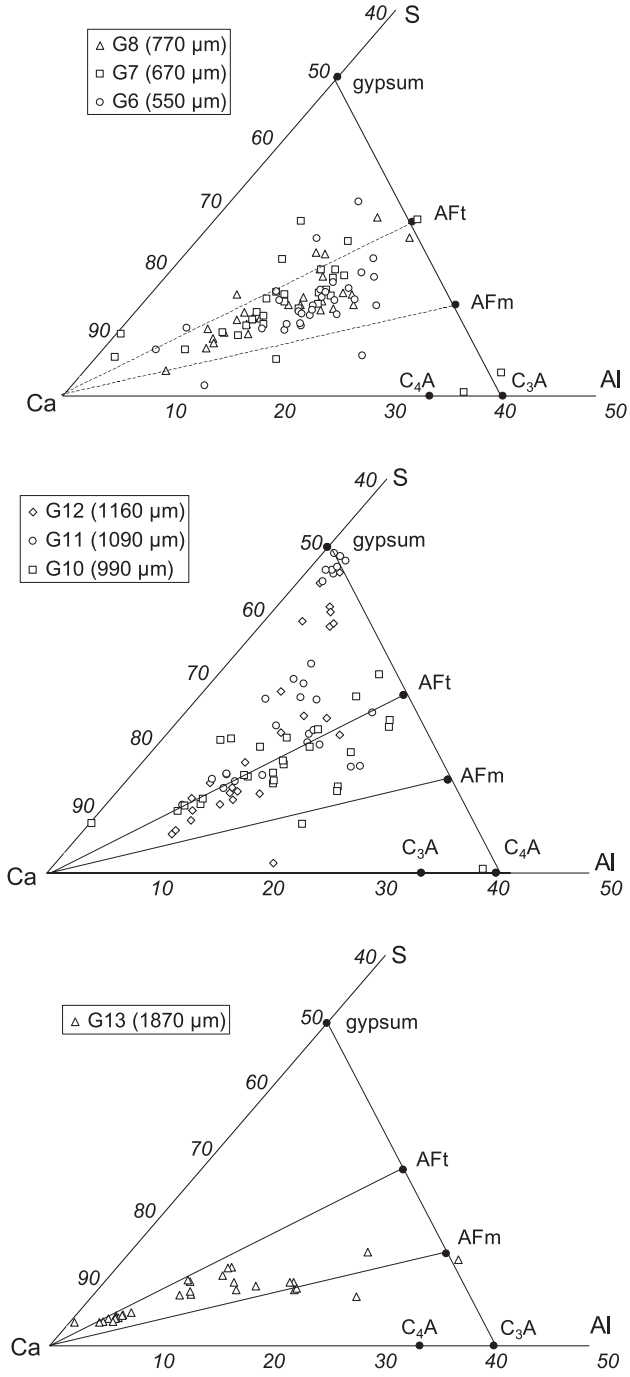

Fig. 6. Part of the system $CaO–Al_2O_3–SiO_2$ in zone 1 (top), zone 2 (center), and zone 3 (bottom).

contrary that gypsum precipitates nearby the portlandite dissolution front (which acts as a calcium source) and that ettringite precipitates homogeneously in the calcium-depleted layer. In addition, these results indicate that gypsum formation occurs prior to crack formation because the profiles were obtained on visually noncracked specimen. To check this distribution, local mass percentages of Ca, S, and Al elements were determined by energy-dispersive spectrometer (EDS) microanalyses of a sample immersed 12 weeks in sodium sulfate. 420 points of analysis were considered, placed on 30 lines perpendicular to the external surface, with a spacing varying between 50 and 200 µm. Results concerning zones 1, 2, and 3 are presented in Fig. 6. They confirm the coexistence of AFt and gypsum in zone 2, and the predominance of AFt in zone 1. Portlandite, monosulfate AFm (C_4ASH_{12}) and ettringite were detected in zone 3 (the sound cement paste). According to Refs. [8,19], the formation of AFt results from the conversion of monosulfate (AFm), the limiting factor for this reaction being the quantity of aluminate ions (Al^{3+}) available, and, therefore, the initial quantity of AFm in the cement paste. The detection of AFm, not possible with XRD owing to its reduced quantity, was therefore of some importance. Overall, these results confirmed the distribution of solid phases in the calcium-depleted layer of the samples as obtained by XRD analyses. The location of gypsum nearby the portlandite dissolution front results probably from the important calcium concentration in this part (provided mainly by the dissolution of portlandite), associated with a sulfate concentration close to the external one (15 mmol/l), owing to the large diffusivity (porosity) of the calcium-depleted layer [2] (zone 1).

3.4. Kinetics of calcium leaching–sulfate attack

According to the XRD profiles (5, 10, 12, and 20 weeks), the position of the portlandite dissolution front (defined as the distance between the external surface and the first point where the height of the portlandite peak is less than 20 Cts/s) presents a square root of time dependency, showing that calcium leaching in sulfate environment (low concentration and controlled pH of 7) is governed by diffusion processes, as it is the case for calcium leaching in pure deionized water [2]. This point is illustrated in Fig. 7. By linear regression, a slope of 0.13 mm/days$^{0.5}$ is obtained for the evolution of the portlandite dissolution front, close to that obtained for standard calcium leaching in pure water [2,3] (0.15 mm/days$^{0.5}$). This latter estimation is based on the layer by layer

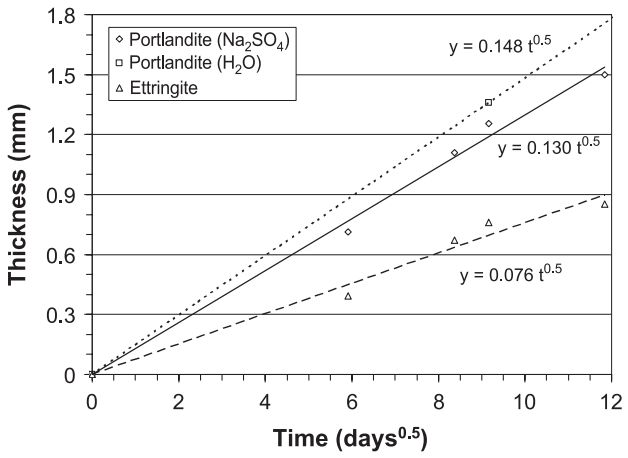

Fig. 7. Evolution of the portlandite dissolution front with time obtained from XRD analysis.

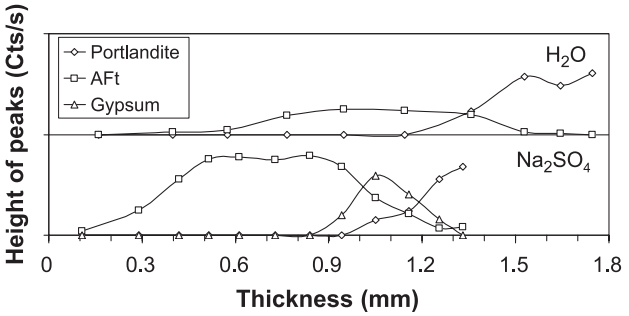

Fig. 8. Phase distribution after 12-week immersion in pure deionized water (H_2O) and sodium sulfate solution (Na_2SO_4).

XRD analysis of a single sample immersed 12 weeks in pure deionized water. The resulting profile is presented in Fig. 8, together with that corresponding to the sample tested 12 weeks in the sodium sulfate solution. The comparison shows that the quantity of formed ettringite is significantly lower, but presents a similar shape. The presence of ettringite during standard calcium leaching tests was formerly shown by Refs. [2,3]. On the contrary, gypsum does not appear in pure deionized water. The size of zone 1 in which ettringite precipitates can also be plotted as a function of the square root of time, showing also a good linearity. This point is illustrated in Fig. 7. This tendency is however not so obvious concerning the size of zone 2, owing to its reduced thickness, even after 20 weeks testing ($\approx$0.2 mm).

3.5. Correlation between cracking and mineralogy

To seek some correlation between mineralogy and cracking, an 8-mm-thick sample immersed 12 weeks in sodium sulfate was prepared for SEM. This specimen presented major cracks parallel to the external surface before removal of water by the freeze-drying technique. It was then polished and resin-impregnated under vacuum. After the preparation, additional microcracks perpendicular to the attacked surface were observed in the sound part of the specimen. A picture of the calcium-depleted layer obtained by SEM is given in Fig. 9, together with the XRD profiles for the sample tested during 12 weeks. The superposition shows obviously that major cracks occur in zone 2 where portlandite, gypsum, and ettringite were detected. Magnification of zone 2 shows veins of gypsum filling cracks subparallel to the external surface, see Fig. 10. Similar observations were reported by Ref. [18] on cubic specimens attacked by sodium sulfate at higher concentrations. No cracks have been observed at this scale in zone 1, in spite of the important quantity of AFt detected by XRD. This is probably a consequence of the simultaneous strong reduction of cement paste stiffness [9] and increase of porosity [2] associated with calcium leaching in this part.

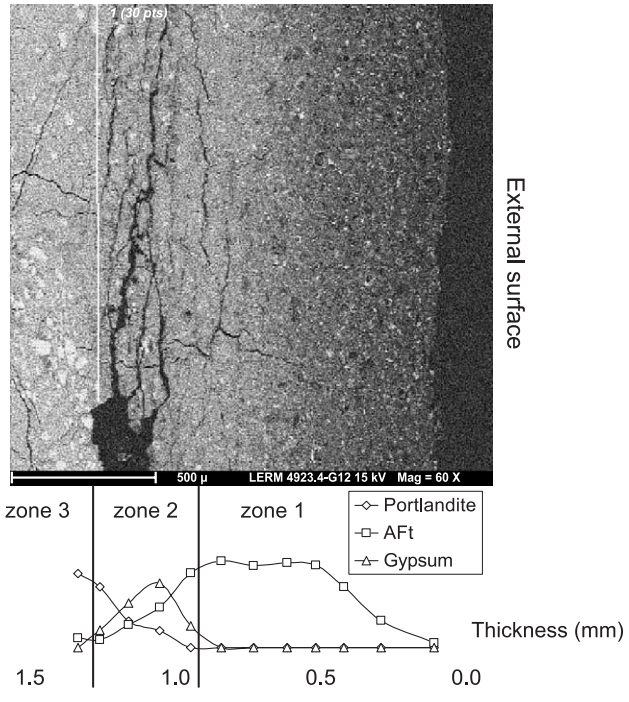

Fig. 9. SEM picture of the cement paste sample after 12-week testing.

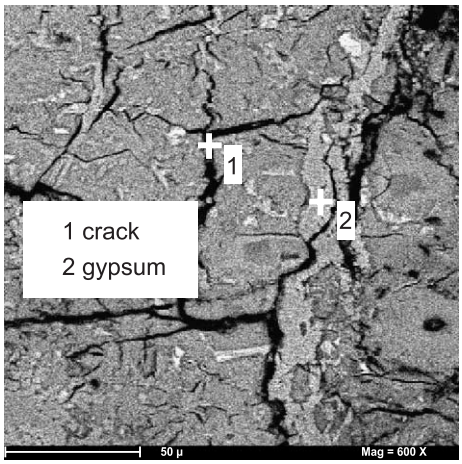

Fig. 10. Magnified SEM picture of zone 2 showing gypsum veins filling the cracks.

4. Conclusions

Experimental results concerning low concentration sodium sulfate attack of portland cement paste (15 mmol/l) have been presented. Periodic chemical and layer by layer XRD/EDS microstructural investigations showed the existence and propagation of two characteristic layers within the calcium-depleted part of the material containing, starting from the external surface:

- mainly ettringite (zone 1),
- ettringite, gypsum, and portlandite (zone 2).

The size of these different layers showed a square root of time dependency, as for the position of the portlandite

dissolution front. These results demonstrate that calcium leaching in sulfate environment presents similar kinetics with respect to calcium leaching in pure deionized water. The presence of sulfates lead however to the precipitation of important quantities of ettringite and gypsum, and consequently to the breakdown of the samples. Cracks were found predominantly in zone 2, perpendicular and parallel to the attacked surface, and partly filled with gypsum. The initiation of cracking and failure of the samples was found to depend significantly on their thickness. The proper estimation of the service life of concrete structures to sulfate attack must therefore account for these marked scale effects.

Acknowledgement

The writers would like to acknowledge the support of this research by the Agence Nationale pour la gestion des Déchets RAdioactifs (ANDRA).

References

[1] M. Buil, E. Revertegat, J.-P. Ollivier, Modelling cement attack by pure water, in: T.M. Gilliam, C.C. Wiles (Eds.), ASTM STP-1123, American Society for Testing and Materials, West Conshohocken, USA, 1992.
[2] F. Adenot, M. Buil, Modelling of the corrosion of the cement paste by deionized water, Cem. Concr. Res. 22 (4) (1992) 489–495.
[3] F. Adenot, J. Maury, C. Richet, Long-term prediction of concrete durability in radioactive waste management: influence of the pH of the aggressive solution, in: A. Al-Manaseer, S. Nagataki, R.C. Joshi (Eds.), Int. Conf. On Eng. Mat., Ottawa, Canada, vol. 2, 1997, pp. 117–128.
[4] D. Planel, Les effets couplés de la précipitation d'espèces secondaires sur le comportement mécanique et la dégradation chimique des bétons [In French], Ph.D. thesis, Collection Les Rapports, ANDRA, France, 2001.
[5] M.D. Cohen, B. Mather, Sulfate attack on concrete—research needs, ACI Mater. J. 88 (3) (1991) 62–69.
[6] P.K. Mehta, Sulfate attack on concrete—a critical review, in: J.P. Skalny (Ed.), Materials Science of Concrete, Am. Ceram. Soc., Westerville, OH, 1992, pp. 104–130.
[7] P.K. Mehta, Sulphate attack on concrete—separating myths from reality, in: V.M. Malhotra (Ed.), 5th CANMET/ACI Int. Conf. on Durability of Concrete, Barcelona, Spain, Supplementary Papers, ACI international, Farmington Hills, USA, 1999, pp. 1–12.
[8] P.W. Brown, H.F.W. Taylor, The role of ettringite in external sulfate attack, in: J. Marchand, J. Skalny (Eds.), Sulfate Attack Mechanisms, Materials Science of Concrete, Am. Ceram. Soc., Westerville, OH, 1998.
[9] C. Carde, R. Francois, Effect of the leaching of calcium hydroxyde from cement paste on mechanical and physical properties, Cem. Concr. Res. 27 (4) (1997) 539–550.
[10] F.H. Heukamp, F.-J. Ulm, J.T. Germaine, Mechanical properties of calcium-leached cement pastes. Triaxial stress states and the influence of the pore pressures, Cem. Concr. Res. 31 (5) (2001) 767–774.
[11] C.F. Ferraris, J.R. Clifton, P.E. Stutzman, E.J. Garboczi, Mechanisms of degradation of portland cement-based systems by sulfate attack, in: K.L. Scrivener, J.F. Young (Eds.), Mechanisms of chemical degradation of cement-based systems, E & FN Spon, London, 1997, pp. 185–192.
[12] P.K. Mehta, Mechanism of Sulfate attack on portland cement concrete—another look, Cem. Concr. Res. 13 (1983) 401–411.
[13] P. Lovera, P. Le Bescop, F. Adenot, G. Li, Y. Tanaka, E. Owaki, Physico-chemical transformations of sulphated compounds during the leaching of highly sulphated cemented wastes, Cem. Concr. Res. 27 (10) (1997) 1523–1532.
[14] J.G. Wang, Sulfate attack on hardened cement paste, Cem. Concr. Res. 24 (4) (1994) 735–742.
[15] P.K. Mehta, Evaluation of sulfate resistance of cements by a new test method, ACI Mater. J. 72 (10) (1975) 573–575.
[16] P.W. Brown, An evaluation of the sulphate resistance of cements in a controlled environment, Cem. Concr. Res. 11 (1981) 719–727.
[17] J.R. Clifton, G. Frohnsdorff, C. Ferraris, Standards for evaluating the susceptibility of cement-based materials to external sulfate attack, in: J. Marchand, J. Skalny (Eds.), Sulfate Attack Mechanisms, Materials Science of Concrete, Am. Ceram. Soc., Westerville, OH, 1998.
[18] R.S. Gollop, H.F.W. Taylor, Microstructural and microanalytical studies of sulfate attack: I. Ordinary portland cement paste, Cem. Concr. Res. 22 (1992) 1027–1038.
[19] P.W. Brown, S. Badger, The distributions of bound sulfates and chlorides in concrete subjected to mixed NaCl, $MgSO_4$, Na_2SO_4 attack, Cem. Concr. Res. 30 (2000) 1535–1542.